

## IONIC STRENGTH DEPENDENCE OF THE HYSTERESIS IN THE POLYRIBOADENYLATE–POLYRIBOURIDYLATE SYSTEM

Melanie SPODHEIM

*Polymer Department, Weizmann Institute of Science, Rehovot, Israel*

and

Eberhard NEUMANN

*Max-Planck-Institut für Biophysikalische Chemie, D-34 Göttingen-Nikolausberg, Germany*

Received 28 May 1974

Revised manuscript received 7 November 1974

The hysteresis observed in cyclic acid–base titrations of the three-stranded polyribonucleotide helix poly(A) · 2 poly(U) strongly depends on ionic strength. For NaCl and at 25°C, hysteresis occurs in the limited concentration range between 0.03 M and 1.0 M (NaCl). The transition points associated with the cyclic conversions between the triple helix and the poly(A) · poly(A) double helix and (free) poly(U) constitute a (pH ionic strength) phase diagram covering the ranges of stability and metastability of the hysteresis system. Variations with NaCl concentration of some hysteresis parameters can be quantitatively described in terms of polyelectrolyte theories based on the cylinder-cell model for rodlike polyions. The results of this analysis suggest that the metastability is predominantly due to electrostatic energy barriers preventing the equilibrium transition of the partially protonated triple helix above a critical pH value.

Ultraviolet absorbance and potentiometric titration data of poly(A) in the acidic pH range can be analyzed in terms of two types of double-helical structures. Spectrophotometric titrations reveal isosbestic wavelengths for structural transitions of poly(A). “Time effects” commonly observed in poly(A) titrations are suggested to reflect helix–helix transitions between the two acidic structures.

### 1. Introduction

Several complexes of the polynucleotides polyriboadenylate, poly(A), and polyribouridylate, poly(U), are known to exhibit thermodynamically metastable states and hysteresis [1–4]. Particularly pronounced is the hysteresis loop found in acid–base titrations of the three-stranded complex poly(A) · 2 poly(U) [5]. This triple helix is obtained if poly(A) and poly(U) are mixed at neutral pH and sufficiently high neutral salt concentration, in the molar ratio of polymers 1:2 [6, 7]. The base residues in the (A · 2U) segments are specifically associated by H-bonds (see fig. 1) and the helical structure is stabilized by base-stacking interactions.

At neutral pH, poly(A) is a partially stacked single strand; at acidic pH the (A) residues of poly(A) are (predominantly) protonated at the N-1 atom [8] and double helical structures are formed [9, 10]. Further-

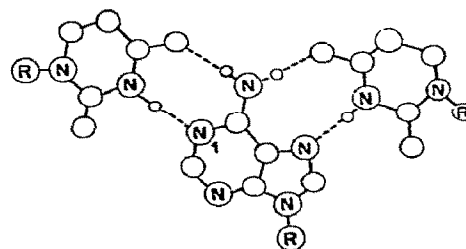


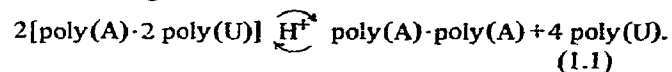
Fig. 1. Schematic representation of the (U · A · U) base pairing in the (A · 2U) segments of poly(A) · 2 poly(U) (after S. Arnott and P.J. Bond, *Nature New Biology* 244 (1973) 99); the N-1 atom of the (A) residue is the protonation site.

more, there is evidence for at least two types of poly(A) · poly(A) double helices, the so-called helix B and helix A [11, 12]; see also the appendix. On the other hand, the (U) residues of poly(U), which at tem-

peratures higher than 20°C is a random coil, are practically not protonated at acidic pH values [13–16].

At constant temperature, the stability of the multi-stranded complexes of the poly(A)–poly(U) system depends not only on the pH value, but also on the salt concentration of the solution. These isothermal dependences have been graphically expressed in phase diagrams [17]. However, these phase diagrams are incomplete because they do not contain regions of metastability. In these regions, the particular complex depends, in addition, on the history of the system, i.e. on the direction in which the state variables have been changed [18]. Details on the thermodynamic aspects of conformational metastability in biopolymers are summarized in a review [19]. In general, metastable states are due to energy barriers which prevent equilibrium transitions; in some cases the resulting non-equilibrium conversions give rise to hysteresis loops.

The loops obtained in acid–base titrations of the poly(A)–poly(U) systems are due to metastability in the triple helix poly(A)·2 poly(U) and are caused by the following “hysteretic” reaction:



It has been suggested that the energy barrier causing the metastability in the poly(A)·2 poly(U) complex is of electrostatic nature [5]. Thus, it is expected that variations in the salt concentration should affect the “hysteretic” transition [eq. (1.1)]. Therefore, acid–base titrations of poly(A)·2 poly(U) have been performed at various concentrations of NaCl. The results of this study permit a detailed analysis of the (A)–2(U) hysteresis in terms of polyelectrolyte theories.

## 2. Materials and methods

### 2.1. Materials

The polymers used in the experiments were polyriboadenylate (K-salt) and polyribouridylate (NH<sub>4</sub>-salt), products of Miles Laboratories, USA.

The polynucleotides were separately dissolved in 0.01 M Na<sup>+</sup>-Cacodylate-NaCl solution (pH 7.1). The concentrations of NaCl used were 0.05 M, 0.1 M, 0.2 M, 0.3 M and 0.5 M NaCl. The concentrations of polynucleotides in solutions were determined spectrophotometrically,

Table 1

Molar extinction coefficients, in 10<sup>3</sup> (M·cm)<sup>-1</sup> units (± 0.1), at 25°C for poly(A) at pH 7, poly(A)·poly(A) in helix B at pH 5.5, poly(U), and poly(A)·2 poly(U) at pH 7, respectively

λ (nm)	ε(A)	ε(AA)	ε(U)	ε(A·2U)
260	10.0	7.5	9.2	17.35
280	3.2	3.0	3.4	7.5
283.5	2.06	2.18	1.85	5.8

metrically, using the extinction coefficients listed in table 1. (These values were determined previously [20] by analysis of nucleotide content following alkaline hydrolysis of polymers [21].)

The polynucleotide solutions were mixed in the molar ratio 1:2 and allowed to equilibrate at 25°C for 10 days. Formation of poly(A)·2 poly(U) was spectrophotometrically observed at the appropriate wavelengths (see subsect. 2.2). The initial residue concentrations of poly(A)·2 poly(U) were  $C = 4 \times 10^{-4}$  M (A·2U) in the potentiometric titrations, and  $C = 2 \times 10^{-5}$  M (A·2U) in the spectrophotometric titrations.

Sterile conditions were maintained during all the experiments.

### 2.2. Methods

#### 2.2.1. Potentiometric titrations

A Radiometer pH-meter 26 and a Metrohm EA-147 combined electrode were used. Solutions were titrated in a thermostated cell with magnetic stirrer. Titrations were started with 6 ml solution. The acid and base, 0.1 N HCl and 0.1 N NaOH, were added from Agla microsyringes with Teflon needles. During the titrations, N<sub>2</sub> was flushed over the titration solution in the sealed titration vessel to prevent CO<sub>2</sub> absorption.

The results of potentiometric titrations are plotted in terms of  $\bar{\alpha}$  as a function of pH; the mean degree of protonation  $\bar{\alpha}$  is defined as the ratio between the number,  $\Delta n$ , of moles of bound protons and the number,  $m$ , of moles of protonation partner (here the (A) residues):  $\bar{\alpha} = \Delta n/m$ . The number of bound protons,  $\Delta n$ , is calculated from the difference in the amounts of acid and base which are necessary to bring the solution of the system, N, to the same pH value as a “blank” solution, B. Titrations are started at pH 7.1 with the same volume,  $v_0$ , for both the system and the “blank”

solution. The formulae for  $\Delta n$  are as follows:

(a) Acid titration:

$$\Delta n = (v_0 + v_H^B)^{-1} [v_0 M_H (v_H^N - v_H^B)],$$

where  $v_H^N$  and  $v_H^B$  are the volumes of acid needed to bring the two solutions to that pH value and  $M_H$  is the molarity of acid.

(b) (Subsequent) base titration:

$$\Delta n = [(v_0 + v_H) + v_{OH}^B]^{-1}$$

$$[v_0 M_{OH} + v_H (M_H + M_{OH})] (v_{OH}^B - v_{OH}^N),$$

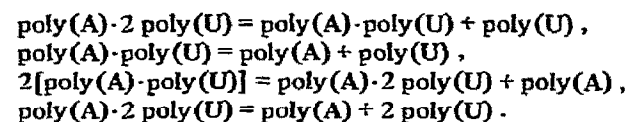
where  $v_H$  is the volume of acid which was added to each solution before base is added,  $v_{OH}^N$  and  $v_{OH}^B$  are the volumes of base needed to bring the solutions to the pH value of interest and  $M_{OH}$  is the molarity of base.

### 2.2.2. Spectrophotometric titrations

A Zeiss PMQ II and the same pH measurement device as for the potentiometric titrations were used. Solutions were titrated in a 1 X 1 X 3 cm quartz cell placed in a thermostated cell-holder with magnetic stirrer. Titrations were started with 2.5 ml solution. The acid and base, 1N HCl and 1N NaOH, were applied from Agla microsyringes in the quartz cell. The method permits simultaneous determination of pH and absorbances.

The results of spectrophotometric titrations are presented as relative absorbance as a function of pH. The relative absorbance, rel.  $A_\lambda$ , at a given wavelength  $\lambda$ , is defined by rel.  $A_\lambda = A_{\lambda, \text{pH}} / A_{\lambda, \text{pH } 7}$ , where  $A_{\lambda, \text{pH}}$  is the absorbance at any pH and  $A_{\lambda, \text{pH } 7}$  the absorbance measured at pH 7. The quantity  $H = \text{rel. } A_\lambda - 1$  represents hyperchromicity when  $H > 0$ , and hypochromicity when  $H < 0$ .

The wavelengths of interest are 260, 280 and 283.5 nm; these are isochromic wavelengths for the four known equilibria of poly(A), poly(U) and poly(A)·poly(U) or poly(A)·2 poly(U) at neutral pH [22–25]:



(a) At 260 nm, the hypochromic change is the same for the association of poly(U) with poly(A) to poly(A)·poly(U) as for the addition of one poly(U) to poly(A)

·poly(U) resulting in poly(A)·2 poly(U); thus, at 260 nm the hypochromic change is the same for the reaction of the first (U) residue with the (A) base as for the second one.

(b) At 280 nm, the absorbance change specifically indicates a change in the equilibrium between poly(A)·2 poly(U) and the separate single strands;

(c) At 283.5 nm, where poly(A)·2 poly(U) is isochromic with its constituents, the formation of poly(A)·poly(U) from poly(A) and poly(U) results in a hyperchromic change.

The use of isochromic wavelengths may decide whether the triple helix converts directly to poly(A)·poly(A) and free poly(U) [according to eq. (1.1)] or via formation of poly(A)·poly(U) as an intermediate. If the transition is direct, it is expected that the absorbance change accompanying reaction (1.1) is the sum of the absorbance changes for the two reactions: poly(A)·2 poly(U) = poly(A) + 2 poly(U) and 2 poly(A) = poly(A)·poly(A). The absolute values for these absorbance changes are known (see ref. [24], table 1 and the appendix).

As outlined elsewhere [19], the metastable states in poly(A)·2 poly(U) are extremely long-lived. There is no observable change over several hours, neither in the absorbance nor in the pH value.

## 3. Results

### 3.1. Potentiometric transitions

An example of potentiometric acid–base titrations of poly(A)·2 poly(U) at 25°C, at two NaCl concentrations 0.06 M and 0.51 M [ $\text{Na}^+$ ] is presented in fig. 2. It is observed that a decrease in pH, from 7 to about 2.5, results in an increase in the mean degree of protonation from 0 to 1, indicating the complete protonation of the (A) residues (which are the predominant protonation partners in this pH range). When the system is titrated from pH 2.5 to pH 7, a different  $\bar{\alpha}(\text{pH})$  curve is traced. We see that the acid  $\bar{\alpha}(\text{pH})$  curve and the base curve form a hysteresis loop. The shape of the loop is different for the different NaCl concentrations. This is mainly due to the differences in the curvatures of the acid branches of the hysteresis loops. Furthermore, both the acid and the base branches are shifted toward lower pH values for higher salt concentrations.

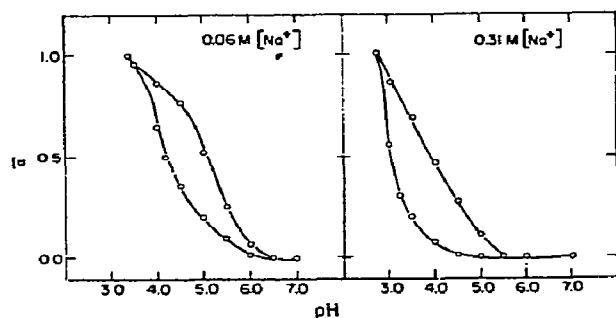


Fig. 2. Hysteresis in the (A)-2(U) system. The mean degree,  $\bar{\alpha}$  of (A) residue protonation as a function of pH for poly(A)-2 poly(U) solutions at two NaCl concentrations, at 25°C. The lower curve is the acid branch and the upper curve is the base branch of the hysteresis loop.

### 3.2. Spectrophotometric titrations

The result of a spectrophotometric acid-base titration of poly(A)-2 poly(U) at 25°C, at two NaCl concentrations is presented in fig. 3. If the pH is decreased from 7 to about 2.5, the relative absorbance at 260 nm increases indicating a structural transition of the system, accompanying the protonation of (A) residues (see fig. 2). As in the potentiometric base titration, addition of base to the acidic solution gives a rel.  $A_{260}$ (pH) curve which is different from the acid titration curve. Here, too, a hysteresis loop is obtained. Similar to the potentiometric hysteresis, the acid and base branches of the spectrophotometric hysteresis loop are shifted to lower pH values for higher salt concentrations. In order to analyse possible intermediate reactions during the acid titration, measurements at  $\lambda = 280$  nm and  $\lambda = 283.5$  nm were performed (fig. 4). It is observed that the relative absorbance at 280 nm increases in the same pH range as rel.  $A_{260}$ . At 283.5 nm a "sudden" increase of absorbance occurs at a certain pH value, denoted  $\text{pH}_c$ ; we see that  $\text{pH}_c$  is different for the various salt concentrations. The maximum changes of the relative absorbances at 260, 280 and 283.5 nm are independent of the salt concentration in the range between 0.06 M and 0.51 M  $[\text{Na}^+]$ :  $H = +0.55$  at 260 nm,  $H = +0.3$  at 280 nm, and  $H = +0.06$  at 283.5 nm.

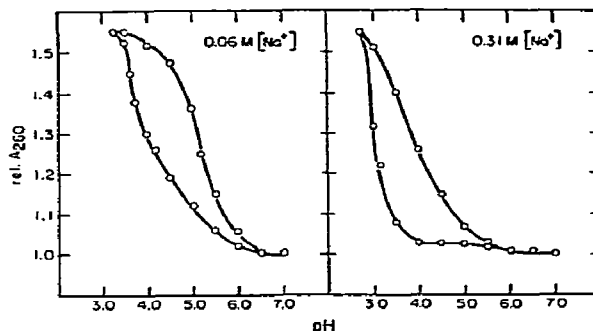


Fig. 3. Relative absorbance at 260 nm, rel.  $A_{260}$ , as a function of pH for poly(A)-2 poly(U) solutions at two NaCl concentrations, at 25°C. See text and fig. 2.

### 3.3. Salt concentration "jumps"

It is found that not only changes in pH induce structural transitions at constant NaCl concentration, but also changes in salt concentration at constant pH. For

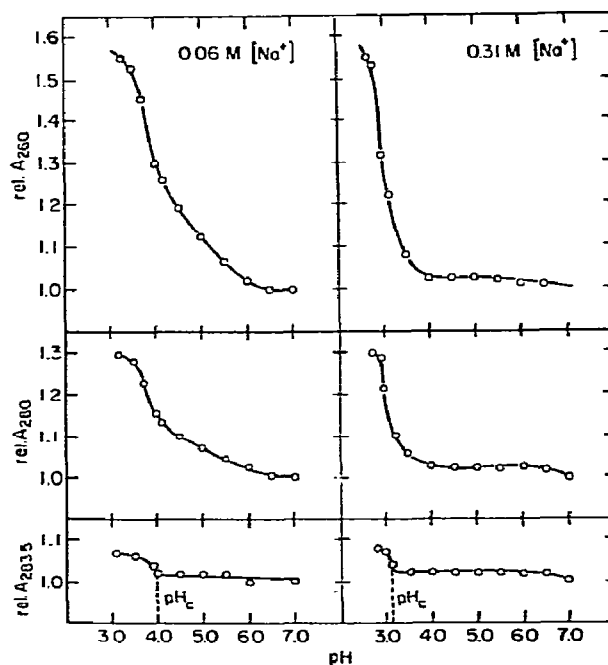


Fig. 4. Relative absorbances, rel.  $A_\lambda$  (acid branch), as a function of pH for poly(A)-2 poly(U) solutions at various NaCl concentrations, at 25°C.

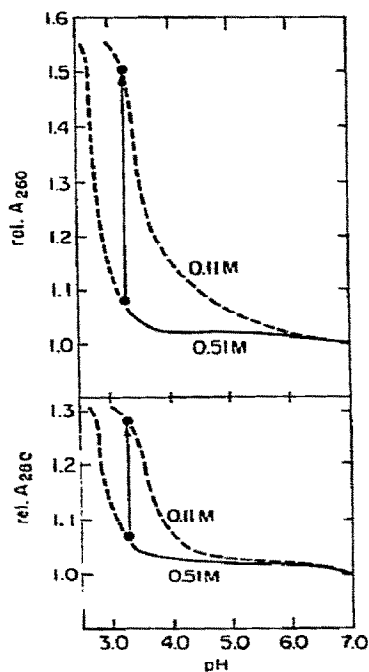


Fig. 5. Changes in the relative absorbances at 260 and 280 nm after a salt concentration "jump" from 0.51 M to 0.11 M  $[\text{Na}^+]$  at pH 3.3, at 25°C; the dotted lines represent the acid titrations of 0.51 M  $[\text{Na}^+]$  and 0.11 M  $[\text{Na}^+]$  solutions, respectively.

instance, at 25°C, the salt concentration of a poly(A)-2 poly(U) solution on the acid branch at pH 3.3 has been decreased from 0.51 to 0.11 M  $[\text{Na}^+]$  (by fast dilution). This "salt jump" leads to an increase in the absorbance at the wavelengths 260, 280 nm (and 283,5 nm) within about 3 min (fig. 5).

In another example, the salt concentration of a solution of the system on the base branch at pH 5.5 was increased from 0.06 M to 0.31 M  $[\text{Na}^+]$ , at 25°C. As a result of this increase, (U) residues are incorporated into base pairs with (A) residues as indicated, e.g. by a decrease in  $\text{rel. } A_{260}$  (see fig. 6). The final values of the absorbance changes are reached only after about 20 h.

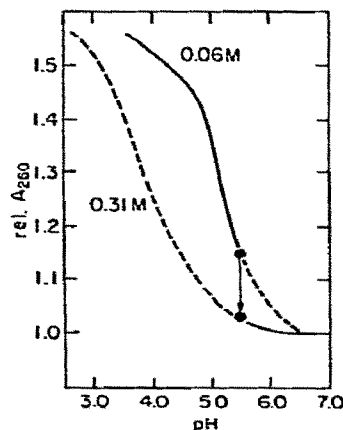


Fig. 6. Change in  $\text{rel. } A_{260}$ , after a salt concentration "jump" from 0.06 M to 0.31 M  $[\text{Na}^+]$  at pH 5.5 on the base branch, at 25°C; the dotted lines represent the base titrations of 0.06 M  $[\text{Na}^+]$  solutions, and 0.31 M  $[\text{Na}^+]$  solutions, respectively.

## 4. Discussion

### 4.1. Hysteresis in poly(A)-2 poly(U) complex

#### 4.1.1. Acid titration

Previous data for the poly(A)-2 poly(U) system have suggested that the formation of poly(A)-poly(A) [eq. (1.1)] is preceded by a (metastable) protonation equilibrium of unpaired (A) residues in the triple helix [5]. In (A-2U) sequences, the potential protonation site (the N-1 atom of adenine) is not "available" for protonation because it is a part of an H-bond between (A) and one of the (U) residues (fig. 1). Since the poly(A)-2 poly(U) complex, however, is characterized by the internal helix-coil equilibrium  $(\text{A} \cdot 2\text{U}) = (\text{A}) + 2(\text{U})$ , where (A) and (U) stretches comprise open ends and loops fluctuating along the complex, protonation can occur at the (A) residues in free ends and loops of the complex. This leads to a partially protonated triple helix. It appears from fig. 4 that if a critical pH value,  $\text{pH}_c$  (corresponding to a critical degree of protonation  $\bar{\alpha}_c$ ) is reached, this intermediate transforms to the protonated poly(A)-poly(A) double helix and poly(U). The conversion is abrupt because poly(A) in the absence of poly(U) forms the double helix in a pH range which is 2 to 3 pH units higher

than the  $\text{pH}_c$  values for the (metastable) triple helix.

It thus seems that in (metastable) poly(A)·2 poly(U) an electrostatic energy barrier (which prevents the (A·A) formation) can be passed if the degree of protonation reaches a critical value. Recently it has been suggested that this energy barrier primarily resides in the electrostatic molecular field properties of the triple helix [26]. In addition, poly(A)·2 poly(U) complexes, even when partially protonated, remain strong polyelectrolytes which repel each other. Since the nucleation of (A·A) stretches requires the approach of two different (A·2U) sequences, repulsion tends to hinder the formation of (A·A) nuclei. For small degrees of protonation, the (AH<sup>+</sup>) stretches in the triple helix are short and nucleation of (A·A) sequences would have to occur within the ionic atmosphere of the neighboring (U) residues. This environment of rather high ionic strength, however, does not favor (A·A) formation. Only when (AH<sup>+</sup>) stretches become long enough to protrude out of the regions of locally high ionic strength and the repulsion between two partially protonated complexes is sufficiently low, (A·A) formation will start.

Before the critical pH is reached the protonation of (A) residues is found to be reversible. Furthermore, at all salt concentrations ranging from 0.06 M to 0.51 M [Na<sup>+</sup>], the first part ( $\text{pH} \geq \text{pH}_c$ ) of the acid branch of the poly(A)·2 poly(U) titration curve can be described by

$$\text{pH} = \text{pK}'_1 + \log[(1-\bar{\alpha})/\bar{\alpha}], \quad (4.1)$$

where  $\text{pK}'_1$  is an apparent  $\text{pK}$  value (see fig. 7). This part of the acid branch corresponds to the metastable protonation equilibrium:  $(\text{A} \cdot 2\text{U}) + \text{H}^+ = (\text{AH}^+) + 2(\text{U})$ . The values of  $\text{pK}'_1$ ,  $\bar{\alpha}_c$ ,  $\text{pH}_c$  for several NaCl concentrations are listed in table 2. It is seen that  $\bar{\alpha}_c$  decreases with increasing NaCl concentration. This is ex-

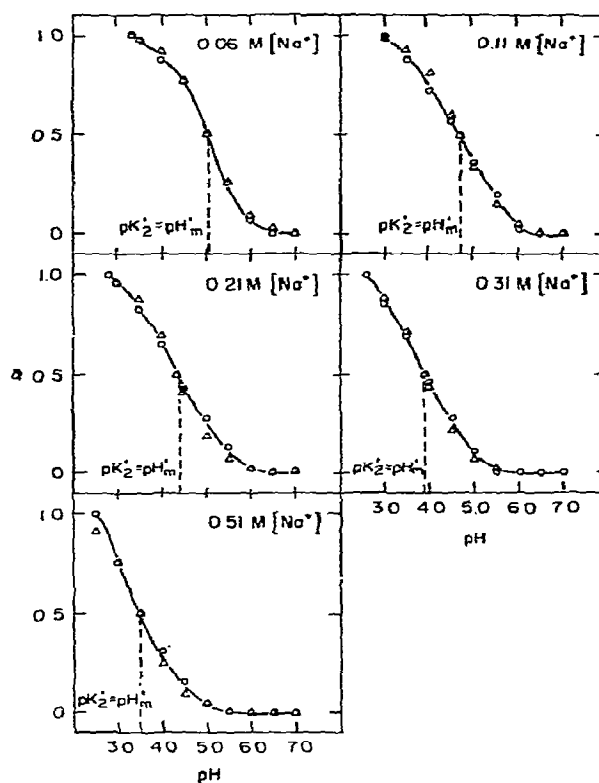


Fig. 7. The mean degree,  $\bar{\alpha}$ , of (A) residue protonation as a function of pH (acid-branch) for poly(A)·2 poly(U) solutions at various NaCl concentrations, at 25°C;  $\text{pH}_m$ , the midpoint of the acid branch, is the pH value corresponding to  $\bar{\alpha} = 0.5$ .  $\circ$ , experimental results;  $\triangle$ , calculated data according to eq. (4.1). (Experimental and calculated curves coincide for  $\bar{\alpha} < \bar{\alpha}_c$  corresponding to  $\text{pH} > \text{pH}_c$ ; see text.)

pected, because at higher salt concentrations the triple helix is more stable and, additionally, repulsions between the triple helices are more reduced. The de-

Table 2  
Hysteresis parameters of the (A)–2(U) system at various NaCl concentrations at 25°C

M[Na <sup>+</sup> ]	0.06	0.11	0.21	0.31	0.51
$\text{pK}'_1$	4.15 ± 0.05	3.6 ± 0.05	3.15 ± 0.05	2.9 ± 0.05	2.65 ± 0.05
$\text{pH}_m$	4.15 ± 0.05	3.6 ± 0.05	3.3 ± 0.05	3.05 ± 0.05	2.85 ± 0.05
$\text{pH}_c(\text{pot})$	4.00 ± 0.05	3.55 ± 0.05	3.35 ± 0.05	3.15 ± 0.05	3.00 ± 0.05
$\text{pH}_c(\text{spec})$	4.00 ± 0.05	3.55 ± 0.05	3.4 ± 0.05	3.15 ± 0.05	3.00 ± 0.05
$\bar{\alpha}_c$	0.60 ± 0.02	0.55 ± 0.02	0.45 ± 0.02	0.40 ± 0.02	0.35 ± 0.02
$\text{pK}'_2 = \text{pH}'_m$	5.05 ± 0.05	4.7 ± 0.05	4.35 ± 0.05	3.90 ± 0.05	3.5 ± 0.05

crease of  $\bar{\alpha}_c$  with increasing NaCl concentration is responsible for the different curvatures of the acid branches (and thus for the different shapes) of the hysteresis loops.

Below the critical pH, i.e. for  $\text{pH} \leq \text{pH}_c$ , the acid titration curve no longer behaves according to eq. (4.1). At  $\text{pH}_c$ ,  $\bar{\alpha}$  increases rather abruptly, indicating (irreversible) formation of (A·A) pairs. If we denote  $\xi$  the extent of reaction (1.1) then, at any pH, the measured degree of protonation  $\bar{\alpha}$  may be expressed by:

$$\bar{\alpha} = (1 - \xi) \alpha_1 + \xi \alpha_2, \quad (4.2)$$

where  $\alpha_1$  is the mean degree of protonation of (A) residues in poly(A)·2 poly(U) and  $\alpha_2$  is the mean degree of protonation in poly(A)·poly(A). (For the pH region  $\text{pH} \geq \text{pH}_c$ , where no (A·A) segments are formed, eq. (4.2) is reduced to  $\bar{\alpha} = \alpha_1$ .)

More direct information about the conformational changes of poly(A)·2 poly(U) during titration can be derived from the spectrophotometric data. As seen in table 2, the  $\text{pH}_c$  values obtained spectrophotometrically agree with those obtained from potentiometric data [fig. 7, cf. eq. (4.1)]. We may thus use measurements at 283.5 nm to determine  $\text{pH}_c$ , conveniently.

It is found that for the acid branch, the total increase in the relative absorbances at 260, 280 and 283.5 nm can be correlated with those calculated for reaction (1.1) using the values of molar extinction coefficients listed in table 1.

If there is no interaction between poly(A)·poly(A) and poly(U), it is expected that the absorbance of this mixture is the sum of the absorbances of the two components. Indeed, for 260 nm the measured absorbance is the same as that calculated for the mixture. However, at 283.5 nm the measured hypochromicity is not equal to that calculated for poly(U) and the *A-form* of poly(A)·poly(A), which is dominant in a poly(A) solution in this pH range. If, however, the absorbance of (A·A) *helix B* is used, the calculated and measured absorbances at 283.5 nm are equal. These observations are reproduced when, for example at pH 4, poly(A) and poly(U) are first separately brought to pH 4, at 0.15 M  $[\text{Na}^+]$  and 20°C, and then mixed in the molar ratio 1:2. Again, at 260 nm the absorbance of the mixture is, indeed, the sum of the absorbance of the constituents, indicating that no detectable (A·2U) sequences were formed. However, at 280 and 283.5 nm, the measured absorbances are larger than

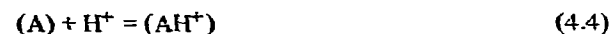
the sum. If, instead, the absorbance of poly(A) in *helix B* is used in the summation, we find that the absorbances of the mixture are equal to the sum of the absorbances of poly(A) and poly(U). Thus, it appears as if the addition of poly(U) causes the conversion of structure A to B. This conversion cannot be seen at 260 nm, because 260 nm is an isosbestic wavelength for the A–B transition (see appendix). Thus, the results of the spectrophotometric titrations and the mixing experiments suggest some as yet unspecified interactions between poly(U) and the poly(A)·poly(A) double helix at low pH.

The increase in absorbance at 260 nm and 280 nm with decreasing pH, clearly indicates that the triple helix transforms according to eq. (1.1) and not via long double helical (A·U) stretches as intermediates.

The absorbance data at 260 and 280 nm may be used to calculate the fraction,  $f$ , of (U) residues decoupled from the base pairing equilibrium:



In the acid pH range this reaction is coupled to the protonation equilibrium:



characterized by  $\alpha_1$ ; for  $\text{pH} \geq \text{pH}_c$ ,  $\alpha_1 = \bar{\alpha}$ .

It is found that at pH values higher than  $\text{pH}_c$ ,  $f$  coincides with  $\bar{\alpha}$ . Thus, the metastable protonation equilibrium is quantitatively described by the coupling between reactions (4.3) and (4.4).

In order to analyze the absorbance changes accompanying the hysteretic reaction [eq. (1.1)], in terms of  $\xi$ , the following relationship may be used:

$$\text{rel. } A_\lambda = [(1-f)(1-\xi) \epsilon_{(\text{A} \cdot 2\text{U})} + (1-\xi) f(\epsilon_{(\text{A})} + 2\epsilon_{(\text{U})}) + \xi(\epsilon_{(\text{A} \cdot \text{A})} + 2\epsilon_{(\text{U})})] / \epsilon_{(\text{A} \cdot 2\text{U})}. \quad (4.5)$$

In eq. (4.5),  $\text{rel. } A_\lambda$  is assumed to be the sum of the contributions of the triple- and double-helical sequences and the single-stranded stretches in the macromolecules [5]. As shown in the appendix, we may set  $\epsilon_{(\text{AH}^+)}$  approximately equal to  $\epsilon_{(\text{A})}$  for  $\lambda = 260$  and 280 nm. If eq. (4.5) is applied to the absorbance changes both at 260 and 280 nm in the metastable range ( $\xi = 0$ ,  $\bar{\alpha} = \alpha_1 = f$ ), it is seen that the same curve is obtained for the extent,  $\xi_a$ , of (A·A) base pair formation on the acid branch. Furthermore,  $\xi_a$  increases from 0 to 1 in a very narrow pH range around  $\text{pH}_c$ ,

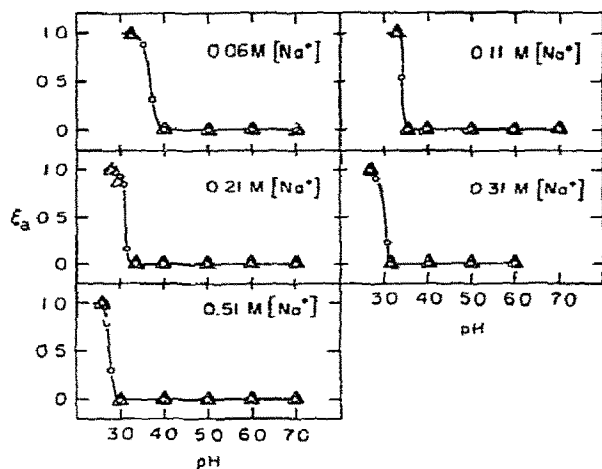
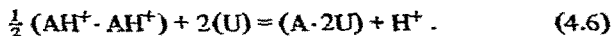


Fig. 8. Extent,  $\xi_a$ , of formation of poly(A)·poly(A) from poly(A)-2 poly(U), as a function of pH, at 25°C (acid branch of hysteresis);  $\circ$ ,  $\xi_a$  calculated from eq. (4.5) using the absorbance data at  $\lambda = 260$  nm.  $\Delta$ ,  $\xi_a$  calculated from eq. (4.5) using the absorbance data at  $\lambda = 280$  nm.

consistent with an abrupt irreversible formation of (A·A) segments from the metastable triple helix (see fig. 8).

#### 4.1.2. Base titration

The reaction occurring along the base branch of hysteresis is



We denote  $\xi_b$  the fraction of (A·A) base pairs on the base branch; we may calculate this quantity from the absorbance data at 260 nm using eq. (4.5). Fig. 9 shows that  $\xi_b$  is gradually decreasing from 1 to 0 with increasing pH from pH 2.5 to 7.

If the changes in the helix-helix transitions of multi-stranded stretches are considered as an intramolecular equilibrium process [5], the pH dependence of the equilibrium constant  $K'_2$  associated with reaction (4.6), may be written as:

$$\text{p}K'_2 = -\log[(1-\xi_b)/\xi_b] + \text{pH} \quad (4.7)$$

It is recalled that in the pH range of interest  $\alpha_1 \cong 0$ ; thus for the base branch of hysteresis, eq. (4.2) reduces to

$$\bar{\alpha} = \xi_b \alpha_2^{(b)} \quad (4.8)$$

As mentioned before, the presence of poly(U) changes the degree of protonation of poly(A). Since  $\alpha_2^{(b)}$  is not known from independent measurements,  $\xi_b$  cannot be calculated from eq. (4.8). We may, however, determine  $\alpha_2^{(b)}$  using  $\xi_b$  obtained from spectrophotometric data. It is seen in fig. 9 that  $\alpha_2^{(b)} = 0.95 \pm 0.05$  for the entire pH range where  $\xi \neq 0$ . In the pH range where  $\alpha_2 \cong 1$  and  $\alpha_1 \cong 0$ , we find  $\bar{\alpha} = \xi_b$  (compare also fig. 2 with fig. 9); thus, the deprotonation curve is a quantitative measure of the pH dependence of the (A·2U) reformation. In consequence almost the entire base branch is expected to be described by the relation:

$$\text{pH} = \text{p}K'_2 + \log[(1-\bar{\alpha})/\bar{\alpha}] \quad (4.9)$$

where  $\bar{\alpha} = \alpha_2^{(b)}$  and  $\text{p}K'_2 = \text{pH}'_m$ , the pH corresponding to  $\bar{\alpha} = 0.5$ .

It is experimentally found that indeed eq. (4.9) accounts for the base branch, except the first part where  $\bar{\alpha} = \alpha_2^{(b)} = 1$  (see fig. 10).

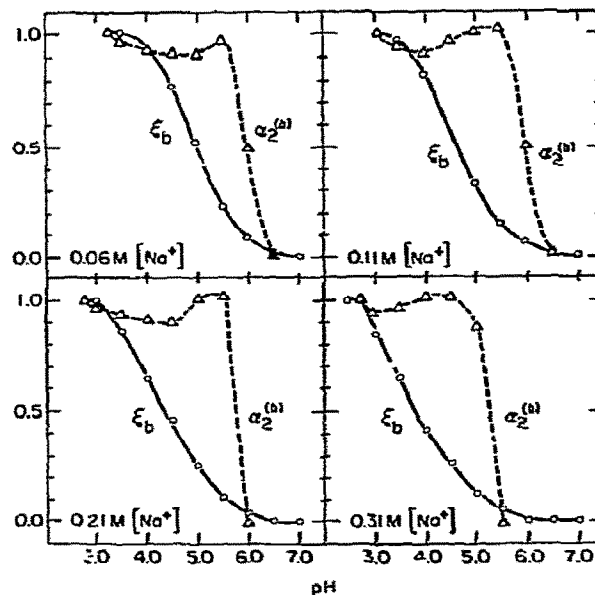


Fig. 9.  $\circ$ , extent of transition,  $\xi_b$ , during the base titration as a function of pH;  $\xi_b$  is calculated using eq. (4.5).  $\Delta$ , degree of protonation  $\alpha_2^{(b)}$ , of (A·A) in the presence of (A·2U) segments;  $\alpha_2^{(b)}$  is calculated from eq. (4.2) using  $\xi_b$ ; see text.

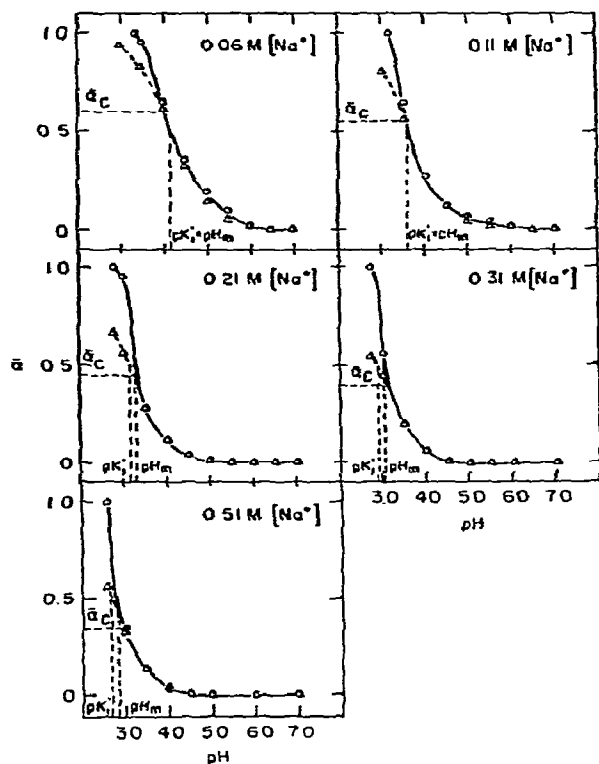


Fig. 10. The mean degree of protonation,  $\bar{\alpha}$ , of the (A) residues in the (A)-2(U) system as a function of pH (base branch) at various NaCl concentrations, at 25°C.  $\circ$ , experimental results;  $\Delta$ , calculated according to eq. (4.9);  $pK_2 = pH_m = pH_{\alpha=0.5}$ .

In the pH range of the base branch of the (A)-2(U) system, the degree of protonation  $\alpha_2$  of poly(A)-poly(A) alone (i.e. in the absence of poly(U)) changes linearly with pH (see appendix, fig. 15). However, in the presence of poly(U), the deprotonation of (A·A) stretches appears to be controlled by the formation of (A·2U) sequences.

According to all these observations, the sequence of events along the base branch may be sketched in the following way: The system at low pH is a mixture of poly(A)·poly(A) and poly(U). When the pH is increased, first poly(A)·poly(A) is deprotonated (as in a solution where only poly(A) is present). Then a pH range is reached where the degree of protonation is

sufficiently low for the nucleation of (A·2U) segments. The “polyelectrolyte effect” of (A·2U) segments causes a local pH that is lower than the pH of the bulk solution. The local environment of higher proton concentration favors the protonated state of (A) residues. Thus, these (A) residues no longer deprotonate as in a solution of poly(A) alone. Instead, with increasing pH,  $\alpha_2^{(b)}$  increases to about 1 and remains close to 1 until around pH 5.5. It is observed that at  $\xi = 0$ ,  $\alpha_2^{(b)}$  decreases (suddenly) to zero. Fig. 11 shows how one may model a junction between (A·2U) and (A·A) stretches of the system at an intermediary pH: almost all the single-stranded (A) segments are deprotonated ( $\alpha_1 \cong 0$ ), and almost all the (A) residues in (A·A) sequences are protonated ( $\alpha_2^{(b)} \cong 1$ ). If  $\xi$  approaches zero, the junction disappears. The pH corresponding to  $\xi \cong 0$  is the critical pH for the base branch. When titrating back to acidic pH, one does not follow the base branch, but one traces an acid branch. Thus, the last part of the base branch appears to be irreversible.

4.1.3. Phase diagram

The results of the acid-base titrations at several NaCl concentrations can be summarized in a phase diagram showing the pH and salt concentration regions of stability and metastability of the system at a given temperature (fig. 12). Under isothermal-isobaric conditions every equilibrium state of the (A)-2(U) system is completely determined by the two parameters

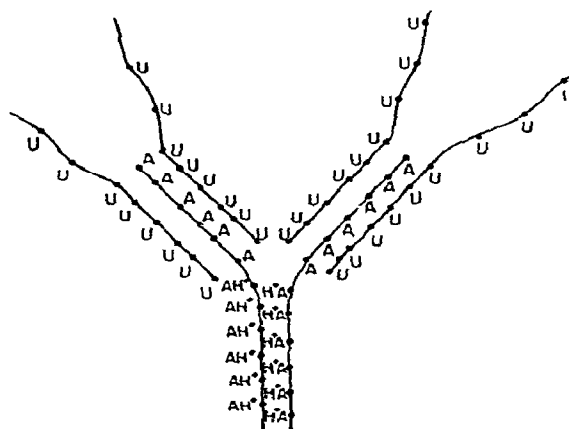


Fig. 11. Model for a section of the (A)-2(U) system in the course of the base titration.

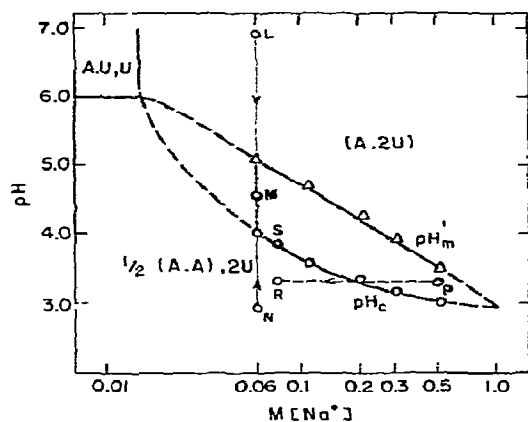


Fig. 12. Phase diagram for the poly(A)-poly(U) system, molar ratio of the polymers 1:2, covering the pH and NaCl concentration ranges of hysteresis, at 25°C. NaCl concentration is given logarithmically.

pH and ionic strength. However, in the domain of hysteresis (shaded area) a complete description of the actual state requires, additionally, knowledge of the history of the system, because a state within a hysteresis field depends on the path on which this area has been reached. For instance, if at a given NaCl concentration the pH of a solution of poly(A)-2 poly(U) is changed from pH 7 to lower pH values, the hysteresis area represents the region of metastability for the triple helix (see L → M). If, however, at the same NaCl concentration, the pH of a solution of poly(A)-poly(A) and poly(U) is increased from a low (e.g. from point N) to a higher pH value (e.g. to point M) the hysteresis area covers a pH range where (A·A), (U) and (A·2U) sequences coexist in equilibrium.

On the other hand, when at a constant pH, the NaCl concentration of a poly(A)-2 poly(U) solution is changed from a high value (e.g. from point P) to a lower one (e.g. to point R), a transition to poly(A)-poly(A) and free poly(U) may be induced. The requirement for such a salt concentration "jump" is that the pH of the (metastable) triple helix solution (e.g. at point P) is lower than the  $pH_c$  (at point S) corresponding to the lower salt concentration. A salt concentration "jump" has been performed according to this requirement. Thus, at P (pH 3.3, 0.51 [Na<sup>+</sup>]), poly(A)-2 poly(U) is in a metastable state. When de-

creasing the salt concentration to 0.11 M [Na<sup>+</sup>], a transition to poly(A)-poly(A) and poly(U) is induced, because  $pH_c$  (0.11 M [Na<sup>+</sup>]) = 3.55 > 3.3.

## 4.2. A theoretical approach to some hysteresis parameters

### 4.2.1. Acid titration

It is recalled that the reaction accompanying the reversible part of the acid titration



represents the coupling between two processes



The corresponding standard free energy changes are  $\Delta_r G_{(a)}^0$  for reaction (4.10),  $\Delta G_{h-c}^0$  for the helix-coil transition [eq. (4.11)], and  $\Delta G_p^0$  for the protonation reaction [eq. (4.12)]. Thus,

$$\Delta_r G_{(a)}^0 = \Delta G_{h-c}^0 + \Delta G_p^0. \quad (4.13)$$

If  $(K'_1)^{-1}$  and  $(K')^{-1}$  are the apparent equilibrium constants for the reactions (4.10) and (4.12), respectively, we have

$$\Delta_r G_{(a)}^0 = -2.3RT \, pK'_1 \quad \text{and} \quad \Delta G_p^0 = -2.3RT \, pK'. \quad (4.14)$$

Introducing eq. (4.14) into eq. (4.13) we obtain

$$pK'_1 = pK' - \Delta G_{h-c}^0 / 2.3RT. \quad (4.15)$$

As mentioned previously, it has been found that for  $pH \geq pH_c$ ,

$$pK'_1 = pH - \log[(1-\bar{\alpha})/\bar{\alpha}]. \quad (4.16)$$

In order to describe the variation of  $pK'_1$  with NaCl concentration, we must consider its influence on  $\Delta G_{h-c}^0$  and on the  $pK'$  of protonation of the (A) residues. In particular we have to take into account that the (A) residues are a part of a polyelectrolyte molecule.

The poly(A)-2 poly(U) macromolecule is a complex of negatively charged polyions (due to the phosphates of the backbone of the polynucleotide chains).

It is known that the titration of a polyelectrolyte with negligible nearest-neighbor interactions between protonated residues can be described by the following equation:

$$\text{pH} = \text{p}K_0 + \log\left[\frac{(1-\bar{\alpha})}{\bar{\alpha}}\right] - 0.434 e\psi/kT, \quad (4.17)$$

where  $K_0$  is the apparent dissociation constant of the isolated monomer residue,  $\psi$  is the potential at the site of protonation and  $\bar{\alpha}$  is the mean degree of protonation. The term  $0.434 e\psi/kT$  introduces the contribution of the polyelectrolyte field to the free energy of protonation. For  $\bar{\alpha} = 0.5$ ,  $\text{pH}_{(\bar{\alpha}=0.5)} = \text{p}K$  and we derive  $\text{p}K = \text{p}K_0 + \Delta\text{p}K$ , where  $\Delta\text{p}K = -0.434 e\psi_{(\bar{\alpha}=0.5)}/kT$ .

It should be noted that the origin of the potential in the case of poly(A)-2 poly(U) is the phosphate residues; thus for low degrees of protonation,  $\psi$  of the N-1 atom of adenine is only slightly affected by changes in  $\bar{\alpha}$ .

Alexandrowicz and Katchalsky [27, 28] derived an expression of  $\Delta\text{p}K$  for polyelectrolyte solutions in which low molecular weight salt is in excess:

$$\Delta\text{p}K = \log\left(\frac{\nu/\pi a^2 h}{n_{\text{R}}^+}\right) + \log\frac{(\lambda-1)^2 - \beta^2}{2\lambda}; \quad (4.18)$$

$$(\lambda = \nu e^2/DhkT),$$

where  $\nu$  = number of negative charges of the polyion,  $a$  = the radius (in cm) of the rod-like macromolecule (cylinder model),  $h$  = the length (in cm) of the cylinder,  $n_{\text{R}}^+$  = the concentration of the positive counterions (molecules/cm<sup>3</sup>) at the boundary surface between the cells (cell-model of polyelectrolyte solution),  $D$  = the dielectric constant of the polyelectrolyte solution,  $\beta$  = integration constant (depending on ionic strength via the Debye-Hückel radius,  $1/\kappa$ ).

We may apply a similar treatment to our case. For reaction (4.12) we write

$$\text{p}K' = \text{p}K_0 + \Delta\text{p}K, \quad (4.19)$$

where  $\text{p}K_0$  is an adenine  $\text{p}K$  of AMP, and  $\Delta\text{p}K$  is the  $\text{p}K$  shift due to the polyionic character of the (A-2U) macromolecule (creating the polyelectrolyte field).

If the ionic strength of the solution is very high, such that practically all the charges are screened, the value of  $\psi$  at the site of protonation is negligibly small. Thus  $\text{p}K' \cong \text{p}K_0$ .

With eq. (4.18) we may calculate  $\Delta\text{p}K$  for any NaCl concentration. Inserting eq. (4.18) into eq. (4.15) one obtains

$$\text{p}K'_1 = \text{p}K_0 + \log\frac{\nu/\pi a^2 h N \times 10^{-3}}{m_s} + \log\frac{(\lambda-1)^2 - \beta^2}{2\lambda} - \frac{\Delta G_{\text{h-c}}^0}{2.3RT}, \quad (4.20)$$

where  $m_s$  is in moles/10<sup>3</sup>cm<sup>3</sup>. (Since the concentration of salt is much higher than the concentration of polymer, we approximate  $n_{\text{R}}^+$  by the salt concentration of the bulk solution.)

The next step is to see how the helix-coil transition (eq. (4.11)) is influenced by the salt concentration. Qualitatively it is obvious that the higher salt concentration will stabilize the triple helix by screening the repulsion between the opposite polyanions of the complex. In the case of DNA a quantitative description of the ionic strength dependence of the free energy of stabilization was given by Manning [29].

Applying a similar approach to our helix-coil transition (4.11) we obtain

$$\Delta G_{\text{h-c}}^0 = \Delta G^0(T) + 1.15 \eta RT \log m_s, \quad (4.21)$$

where  $\eta = \xi_c^{-1} - \xi_h^{-1}$  ( $\xi = e^2/DkTb$ , where  $b$  is the average spacing of the projection of the charged groups onto the axis of the polyion for the coil and helix state, respectively),  $\Delta G^0(T)$  is a reference value ( $\Delta G^0(T) = \Delta G_{\text{h-c}}^0$  for the transition in 1 M salt solution). Introducing (4.21) into (4.20) we obtain

$$\text{p}K'_1 = \text{p}K_0 + \log\frac{\nu}{\pi a^2 h N \times 10^{-3}} + \log\frac{(\lambda-1)^2 - \beta^2}{2\lambda} - \frac{\Delta G^0(T)}{2.3RT} - (1 + 0.5\eta) \log m_s. \quad (4.22)$$

Denoting  $\Delta\text{p}K_1$  the NaCl concentration dependent term, one may write

$$\Delta\text{p}K_1 = \text{p}K'_1 - \text{p}K_1^* = \log\frac{(\lambda-1)^2 - \beta^2}{2\lambda} - (1 + 0.5\eta) \log m_s, \quad (4.23)$$

where  $\text{p}K_1^*$  includes the NaCl concentration-independent contributions. For our particular case, on average,  $\bar{b}_c \cong 6.8$  Å, and  $\bar{b}_h \cong 1.1$  Å, thus one obtains  $\eta = 0.84$ , and  $\lambda = 6$ . The values of  $\beta^2$  are obtained by interpolating from a plot of  $\beta^2$  as a function of  $\kappa a$  at constant  $\lambda$  [27]. It is found that  $\log\{[(\lambda-1)^2 - \beta^2]/2\lambda\}$  is also a linear function of  $\log m_s$ , thus

$$\Delta\text{p}K_1 = \text{const}' \cdot \log m_s - (1 + 0.5\eta) \log m_s = \text{const} \cdot \log m_s. \quad (4.24)$$

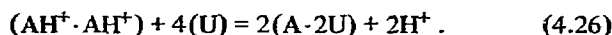
From eqs. (4.23) and (4.24) it is derived that under isothermal-isobaric conditions

$$d\Delta pK_1/d \log m_s = d pK'_1/d \log m_s = \text{const.} \quad (4.25)$$

In fact, the experimental  $pK'_1$  values are linearly dependent on  $\log m_s$ , with  $dpK'_1/d \log m_s \approx 1.5 \pm 0.1$  (see fig. 13b). Furthermore, the calculated  $\Delta pK_1$  values are also linearly dependent on  $\log m_s$  with  $d\Delta pK_1/d \log m_s = 1.6$  (see fig. 13a). Thus, within experimental accuracy, eq. (4.25) is valid over the entire range of NaCl concentrations in which hysteresis is observed.

#### 4.2.2. Base titration

It is recalled that the reaction accompanying the base titration is



This reaction may be formally split into three reactions: a (small) opening of the double strand [eq. (4.27)], deprotonation of  $(\text{AH}^+)$  [eq. (4.28)] and formation of  $(\text{A} \cdot 2\text{U})$  segments [eq. (4.29)].



The corresponding standard free energy changes are:  $\Delta_1 G_{(b)}^0$  per mole residue for reaction (4.26);  $\Delta G_{(\text{A} \cdot \text{A})}^0$  per mole (A) residue for reaction (4.27);  $\Delta G_{\text{dep}}^0$  for the deprotonation reaction (4.28);  $\Delta G_{\text{c-h}}^0$  for the helix formation (4.29):

$$\Delta_1 G_{(b)}^0 = \Delta G_{\text{dep}}^0 + \Delta G_{\text{c-h}}^0 + \Delta G_{(\text{A} \cdot \text{A})}^0 \quad (4.30)$$

For eq. (4.26) we have

$$\Delta_1 G_{(b)}^0 = 2.3 RT \text{pH}'_m \quad (4.31)$$

Since  $\bar{\alpha} \cong \xi$ , we obtain  $\text{pH}'_m = \text{p}K'_2$  (where  $K'_2$  is the apparent equilibrium constant for reaction (4.26)).

If  $K''$  is the apparent equilibrium constant of reaction (4.28), we have

$$\Delta G_{\text{dep}}^0 = 2.3 RT \text{p}K'' \quad (4.32)$$

Introducing eqs. (4.32) and (4.31) into eq. (4.30) (and using  $\Delta G_{\text{c-h}}^0 = -\Delta G_{\text{h-c}}^0$ ) one obtains

$$\text{pH}'_m = \text{p}K'' - \frac{\Delta G_{\text{h-c}}^0}{2.3RT} + \frac{\Delta G_{(\text{A} \cdot \text{A})}^0}{2.3RT} \quad (4.33)$$

At pH values around  $\text{p}K''$  the deprotonation of (A) residues most likely occurs in junctions, i.e. near  $(\text{A} \cdot 2\text{U})$  segments. Fig. 14 shows the model (cf. fig. 11) for such a junction between stretches of  $(\text{A} \cdot 2\text{U})$  segments and a stretch of  $(\text{A} \cdot \text{A})$  segments. We now denote I the cylinder of the  $(\text{A} \cdot 2\text{U})$  segments and II the cylinder of the protonated  $(\text{A} \cdot \text{A})$  segments. Furthermore, we assume that a given (A) residue is either in

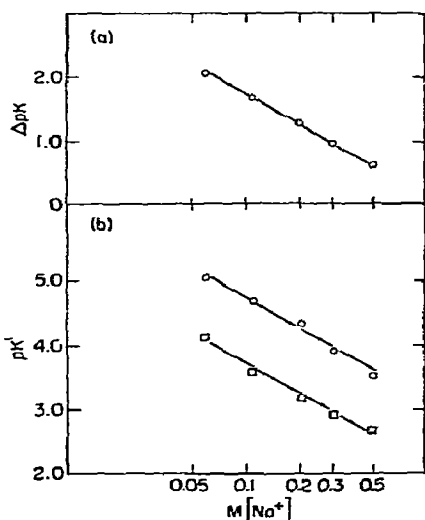


Fig. 13. Dependence on NaCl concentration (a) of  $\Delta pK$ ; calculated according to eq. (4.23); (b) of  $pK'$ ;  $\circ$ ,  $pK'_1$ , derived from experimental data of the acid titration (fig. 7);  $\square$ ,  $\text{pH}'_m$  derived from experimental data of the base titration (fig. 10).

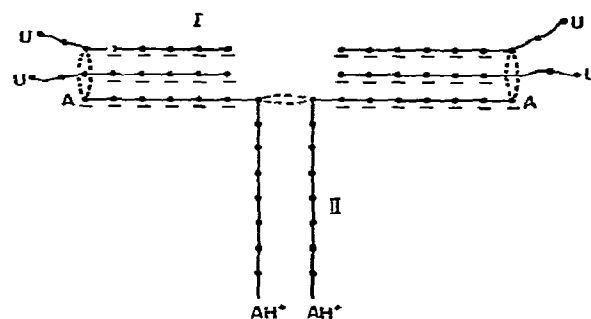


Fig. 14. Scheme for a junction between  $(\text{A} \cdot \text{A})$  and  $(\text{A} \cdot 2\text{U})$  cylinders.

(I) or in (II) except the few which may be single-stranded at the junction between both cylinders. Whereas cylinder I is highly negatively charged, cylinder II has almost no net charge, because at  $\alpha_2^{(b)} \cong 1$ , the protonated (A) residues compensate the charges of the phosphate residues. Therefore, the potential at the site of deprotonation of (A) is assumed to be mainly determined by the charges of cylinder I.

The apparent  $pK$  for the deprotonation reaction of (A) at such a junction may be split into an intrinsic  $pK_0$  and a  $\Delta pK$ , i.e.,  $pK'' = pK_0 + \Delta pK$ . The value of  $\Delta pK$  may be calculated as previously [see eq. (4.18)] neglecting interactions between different junctions.

Thus, analogous to eq. (4.22) we have for the base branch:

$$pH'_m = pK_0 + \log \frac{\nu}{\pi a^2 h N \times 10^{-3}} + \log \frac{(\lambda-1)^2 - \beta^2}{2\lambda} - \frac{\Delta G_{h-c}^0 - \Delta G_{(A \cdot A)}^0}{2.3RT} - (1 + 0.5\eta) \log m_s. \quad (4.34)$$

To a good approximation,  $\Delta G_{(A \cdot A)}^0$  is independent of salt concentration, since  $\Delta G_{(A \cdot A)}^0$  refers to the "rupture" of H-bonds and unstacking of the protonated electroneutral (A) residues without changing the degree of protonation.

Denoting by  $\Delta pK_2$  the NaCl concentration-dependent terms, one may write:

$$\Delta pK_2 = pH'_m - pK_2^* = \log \frac{(\lambda-1)^2 - \beta^2}{2\lambda} - (1 + 0.5\eta) \log m_s, \quad (4.35)$$

where  $pK_2^*$  includes all the contributions independent of salt concentration. From a comparison of eq. (4.35) with eq. (4.23) we see that  $\Delta pK_2 = \Delta pK_1$ .

Thus, from eqs. (4.35) and (4.24) we derive

$$dpH'_m/d\log m_s = d\Delta pK_2/d\log m_s = d\Delta pK_1/d\log m_s = \text{const.} \quad (4.36)$$

Fig. 13 shows that the experimental  $pH'_m$  values are indeed linearly dependent on  $\log m_s$ , yielding  $dpH'_m/d\log m_s = 1.5 \pm 0.1$ . The calculated values for  $\Delta pK_2$  ( $= \Delta pK_1$ ) also depend linearly on  $\log m_s$  with  $d\Delta pK_2/d\log m_s = d\Delta pK_1/d\log m_s = 1.6$  (see fig. 13a). Thus, eq. (4.36) quantitatively accounts for the salt concentration dependence of the  $pH'_m$  values.

In summary, the salt concentration dependence of the  $pK$  values for the metastable protonation equilib-

rium (first part of the acid branch of hysteresis) as well as for the equilibrium transition (base branch of hysteresis) can be quantitatively expressed in terms of the cylinder-cell model of polyelectrolyte theory. Finally, our model for the hysteresis observed in acid-base titrations of the poly(A)-2 poly(U) complex describes the transition behavior in the entire salt-concentration range in which hysteresis occurs. Thus, the present analysis substantiates that the metastability of the triple helix is predominantly caused by an energy barrier which is electrostatic in nature.

#### Acknowledgements

The present study was initiated under the guidance of the late Aharon Katchalsky. We thank I. Miller and A. Silberberg for critical comments and gratefully acknowledge a grant by the Stiftung Volkswagenwerk, Germany, and an EMBO fellowship to E.N.

#### Appendix

##### *Structural transitions of polyriboadenylate in the acidic pH range*

The analysis of the hysteresis observed in the (A)-2(U) system requires proton binding and absorbance data of poly(A) at acidic pH values.

It has been shown by X-ray diffraction studies on fibers drawn from acidic solutions of poly(A) that, depending on pH, two types of double helical structures, B and A, or a mixture of both, may exist [11]. Structure B (with 10 nucleotides in one turn of the helix, spaced at 3.6 Å) has been attributed to the less protonated states and structure A (with 8.4 nucleotides in one turn of the helix, spaced at 3.8 Å), to the more protonated one. It has been suggested that the "more extended" character of structure A is caused by repulsion between the protons on adjacent N-1 positions; this repulsion may open up the molecule. In both helices, the interaction between the two strands involve H-bonding, base stacking and electrostatic contributions. Specifically, electrostatic attraction between the protonated (i.e. positively charged) bases of one strand and the negatively charged phosphates of the opposite strand, is a stabilizing factor of

the polyionic complex [9].

Optical rotatory dispersion studies suggest that, also in solution, poly(A) exhibits two different acidic structures [12]. It has been reported that "spectrophotometric titrations do not reveal the presence of the two forms". The absorbance range covered in that study was from 250 to 270 nm [12]. If, however, the optical measurements are performed in the range from 260 to 285 nm, as in the present work, the absorbance data do suggest the presence of two acidic forms. Furthermore, the proton binding curves of poly(A) can also be analyzed in terms of the two structures.

#### Proton binding curves of poly(A)

Fig. 15 shows the results of potentiometric titrations of poly(A) at various NaCl concentrations at 25°C. It is seen that with increasing salt concentration the proton binding curves,  $\bar{\alpha}(\text{pH})$ , are shifted to lower pH values. In the pH range of the single-to-double strand transition, the slope of the  $\bar{\alpha}(\text{pH})$  curve depends on the ionic strength of the solution. An increase of salt concentration causes a decrease of the slope. Due to the different geometry of the poly(A)-poly(A) helix types we may assume that the two structures have different proton binding curves. If the decrease in pH causes the conversion of B to A, then in the course of the acid titration we pass from the protonation curve of B to that of A. Thus, the slope of the actual proton binding curve of poly(A) is determined by the distance between the  $\bar{\alpha}(\text{pH})$  curve of B and that of A (on the pH scale). Because the distances between the charged

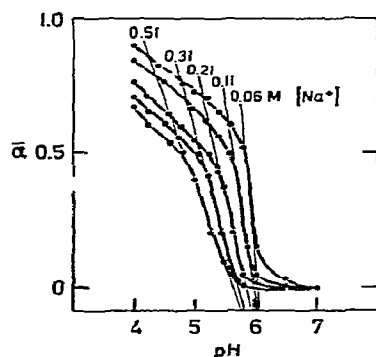


Fig. 15. Proton binding curves,  $\bar{\alpha}(\text{pH})$ , of poly(A) at various NaCl concentration at 25°C; (A) residue concentration is  $8 \times 10^{-4}$  M (A) at pH 7.

groups of the two helical conformations are different, the proton binding curves of B and A may be differently affected by the ionic strength of the solution. It is recalled that B is a more compact structure than A. Thus, the "inner salt bridges" between phosphates and protonated (A) bases of opposite strands are more effectively "buried" in the interior of the double helix B than in the interior of helix A. The "more extended" structure A is therefore expected to be more sensitive to variations in salt concentration than structure B. Hence, with increasing salt concentration, the  $\bar{\alpha}(\text{pH})$  curve of A is shifted to lower pH values to a larger extent than the  $\bar{\alpha}(\text{pH})$  curve of B. Therefore, the distance between the  $\bar{\alpha}(\text{pH})$  curves of the two (separate) structures is larger for higher than for lower salt concentration. Consequently, at higher salt concentration the slope of the actual proton binding curve of poly(A) is smaller than at lower salt concentration. Thus, the assignment of different pK values for the two helices accounts for the observed protonation curves (fig. 15).

#### Drifts of pH with time in the acidic pH range

A further experimental observation is the following: a drift in pH with time was found in the region between pH 5.55 and pH 4. When adding acid, there is no immediate decrease of pH. After some seconds the pH decreases and within about 5 min the pH change seems to level off. This drift of pH with time may be modelled also in terms of the B-to-A transition. If, for example, one adds acid to poly(A) in state M (see fig. 16), first protons are bound to structure B, and one obtains a short-lived metastable state N.

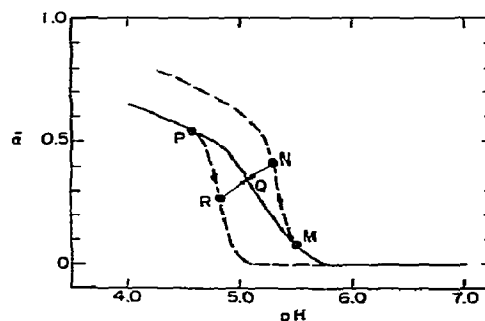


Fig. 16. Scheme for the interpretation of "time effects" in the acid-base titration of poly(A); see text.

Subsequently, structure B partially transforms to structure A. In the course of this transition protons are released because at that pH, structure A binds less protons than structure B. This results in a drift of pH to lower values. The stable state, reached by the system only after some minutes, is state Q. A similar observation of "time-dependent pH values" has been reported for the titration of poly(A) from acidic to neutral pH values (at low ionic strength and low temperature) [30]. This observation may be modelled in terms of a slow A-to-B transition. If, for example, one adds alkali to poly(A) in state P, first the protons are released from structure A and one obtains a short-lived metastable state R. Subsequently, structure A partially transforms to structure B. During this transition protons are taken up because at that pH, structure B binds more protons than structure A. This results in a drift of pH to higher values. The stable state, reached only after some time, is state Q.

#### Spectrophotometric acid titration of poly(A)

For the analysis of the A-2U hysteresis, the wavelengths 260, 280 and 283.5 nm are of particular interest. Therefore the spectrophotometric titration of poly(A) has been performed in the same wavelength range. The results of the absorbance measurements are presented in fig. 17. It is seen that three pH regions (separated by dashed lines) can be distinguished:

(a) At  $\lambda = 260$  nm, the absorbance does not change between pH 7 and pH 6.25. Between pH 6.25 and pH 5.55 the absorbance decreases. This decrease corresponds to  $H = -0.25$ . For pH values lower than 5.55, there is no further change of absorbance at this wavelength.

(b) At  $\lambda = 280$  nm, no absorbance change is observed between pH 7 and pH 6.25. Between pH 6.25 and pH 5.55 one finds a value of  $H = -0.08$ ; decreasing further the pH one observes that  $A_{280}$  also decreases. The total hypochromicity between pH 6.25 and pH 4 is  $H = -0.13$ .

(c) At  $\lambda = 282$  nm, no absorbance change is observed between pH 7 and pH 5.55. If the pH is lowered from pH 5.55 to pH 4, a hypochromicity of  $H = -0.09$  is found.

(d) At  $\lambda = 283.5$  nm, no absorbance change is observed between pH 7 and pH 6.25. An increase in absorbance of  $H = +0.06$  is obtained between pH 6.25 and pH 5.55. A further decrease in pH leads to a de-

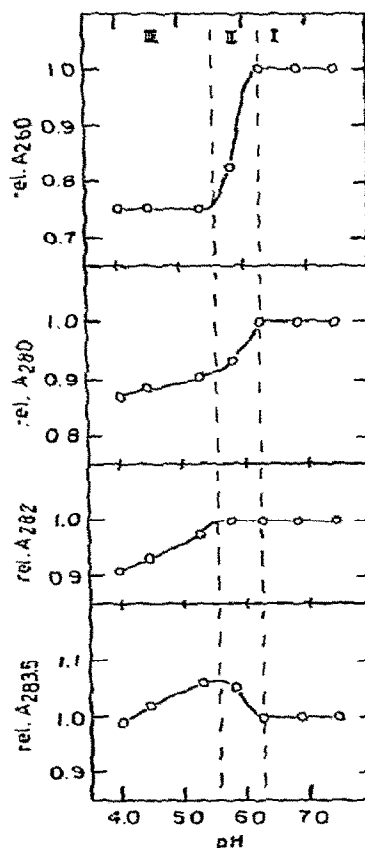


Fig. 17. Relative absorbances of poly(A) in 0.01 M  $\text{Na}^+$  cacodylate, 0.1 M NaCl, at 25°C, as a function of pH (at a poly(A) residue concentration of  $8 \times 10^{-5}$  M (A) at pH 7).

crease in absorbance, so that the absorbance at pH 4 is equal to the absorbance at pH 7.

We denote the three different pH regions by: (i) from pH 7 to pH 6.25; (ii) from pH 6.25 to pH 5.55; (iii) from pH 5.55 to pH 4. Region I corresponds to single-stranded poly(A). In this region there are no absorbance changes at the wavelengths used, although the proton binding curves show that (A) residues are already protonated. Since at these wavelengths  $\epsilon_{(\text{AH}^+)}$  is approximately equal to  $\epsilon_{(\text{A})}$ , there is apparently no detectable change in single-strand base stacking upon protonation of (A) residues. The transition from the single-stranded poly(A) to the double-stranded

helix B occurs in region II. This transition gives rise to changes in the absorbance spectrum of poly(A). For example, the absorbance decreases at 260 and 280 nm, but it increases at 283.5 nm. However, no change in absorbance is seen at 282 nm. Thus, 282 nm is an isosbestic wavelength for the transition of poly(A) from single strand to helix B. In region III, structure B transforms to structure A. Relative to region II, this transition gives rise to a decrease in absorbance at 280, 282 and 283.5 nm, but no change is seen at 260 nm. Thus, 260 nm is an isosbestic wavelength for the transition of poly(A) from helix B to helix A. The use of isosbestic wavelengths may be exemplified in the following way: if in a system where poly(A) is a reaction partner, two processes occur concomitantly, one of them being, e.g., the helix B-helix A conversion, the other reaction may be specifically followed at 260 nm. On the other hand, because 260 nm was the only wavelength used in previous A-2U hysteresis studies [5], the observation that poly(A)-poly(A) in the presence of poly(U) is apparently in form B could not be made.

When potentiometric and spectrophotometric titrations data are combined, a relationship between the degree of protonation and the acidic structures of poly(A) is obtained. The potentiometric titration shows that at 0.11 M  $[Na^+]$  and 25°C, the pH value corresponding to  $\bar{\alpha} = 0.5$  is 5.55 (cf. fig. 15). It is seen from the spectrophotometric data of poly(A) for the same conditions that at pH 5.55 the conversion of B to A starts to contribute to the absorbance (cf. fig. 17). This indicates that at 0.11 M  $[Na^+]$  and 25°C, structure A develops when on average one (A) per (A·A) base-pair is protonated. This finding is in agreement with the results of ORD studies [12].

In summary, ultraviolet spectrophotometric and potentiometric titrations of poly(A) in solutions of various NaCl concentrations in the acidic pH range can be analyzed in terms of two types of double-helical structures (in line with the interpretation of X-ray diffraction and ORD data). Furthermore, the spectrophotometric titrations show some isosbestic wavelengths for the structural transitions of poly(A). "Time effects" commonly observed in titrations of poly(A) are suggested as being caused by slow transitions between the two acidic structures.

## References

- [1] R.C. Warner, *Fed. Proc.* 15 (1956) 379.
- [2] R.F. Beers and R.F. Steiner, *Nature* 181 (1958) 30; *Biochim. Biophys. Acta* 33 (1959) 470.
- [3] R.A. Cox, *Biochim. Biophys. Acta* 68 (1963) 401.
- [4] V. Vetter and W. Guschlbauer, *Arch. Biochem. Biophys.* 148 (1972) 130.
- [5] E. Neumann and A. Katchalsky, *Ber. Bunsenges. Phys. Chemie* 74 (1970) 868.
- [6] G. Felsenfeld, D.R. Davies and A. Rich, *J. Am. Chem. Soc.* 79 (1957) 2023.
- [7] G. Felsenfeld and H.T. Miles, *Ann. Rev. Biochem.* 36 (1967) 407.
- [8] W. Cochran, *Acta Cryst.* 4 (1951) 81.
- [9] J.R. Fresco and P. Doty, *J. Am. Chem. Soc.* 79 (1957) 3928.
- [10] A. Rich, D.R. Davies, F.H.C. Crick and J.D. Watson, *J. Mol. Biol.* 3 (1961) 71.
- [11] J.T. Finch and A. Klug, *J. Mol. Biol.* 46 (1969) 597.
- [12] A.J. Adler, L. Grossman and I.D. Fassman, *Biochemistry* 8 (1969) 3846.
- [13] D.H. Rammner, A. Deik and C.W. Abell, *Biochemistry* 4 (1965) 2002.
- [14] J.C. Thrierr and M. Leng, *Biochim. Biophys. Acta* 182 (1969) 575.
- [15] J.C. Thrierr, M. Dourlant and M. Leng, *J. Mol. Biol.* 58 (1971) 815.
- [16] L.D. Inners and G. Felsenfeld, *J. Mol. Biol.* 50 (1970) 373.
- [17] J. Massoulié, *Europ. J. Biochem.* 3 (1968) 439.
- [18] D.H. Everett in E.A. Flood: *The solid gas interface*, vol. 2 (Marcel Dekker, New York, 1967) p. 1055.
- [19] E. Neumann, *Angew. Chem. Internat. Edit.* 12 (1973) 356.
- [20] M. Spodheim, Progress Report, Weizmann Institute of Science, Israel (1972).
- [21] J.R. Fresco and B.M. Alberts, *Proc. Natl. Acad. Sci., USA* 46 (1960) 311.
- [22] C.L. Stevens and G. Felsenfeld, *Biopolymers* 2 (1964) 293.
- [23] J. Massoulié, R. Blake, L. Klotz and J. Fresco, *Comptes Rendues Acad. Sci. Paris* 259 (1964) 3104.
- [24] R.D. Blake and J. Fresco, *J. Mol. Biol.* 19 (1966) 145.
- [25] R.D. Blake, J. Massoulié and J.R. Fresco, *J. Mol. Biol.* 30 (1967) 291.
- [26] G. Weissbuch and E. Neumann, *Biopolymers* 12 (1973) 1479.
- [27] Z. Alexandrowicz and A. Katchalsky, *J. Polymer Sci. A1* (1963) 3231.
- [28] A. Katchalsky, Z. Alexandrowicz and O. Kedem, in: *Chemical physics of ionic solutions*, ed. B.E. Conway and R.G. Barrads (Wiley, New York, 1966) p. 295.
- [29] G. Manning, *Biopolymers* 11 (1972) 937.
- [30] N.D. Holcomb and S.N. Timasheff, *Biopolymers* 6 (1968) 513.